Research in Astron. Astrophys. **2012** Vol. **12** No. **11**, 1475–1485
http://www.raa-journal.org *http://www.iop.org/journals/raa*

Research in Astronomy and Astrophysics

The connection between radio and γ-ray emission in Fermi/LAT blazars *

Xu-Liang Fan[1,2,4], Jin-Ming Bai[1,2], Hong-Tao Liu[1,2], Liang Chen[3] and Neng-Hui Liao[1,2,4]

[1] National Astronomical Observatories / Yunnan Observatory, Chinese Academy of Sciences, Kunming 650011, China; *fxl1987@ynao.ac.cn; baijinming@ynao.ac.cn*
[2] Key Laboratory for the Structure and Evolution of Celestial Objects, Chinese Academy of Sciences, Kunming 650011, China
[3] Key Laboratory for Research in Galaxies and Cosmology, Shanghai Astronomical Observatories, Chinese Academy of Sciences, Shanghai 200030, China
[4] Graduate University of Chinese Academy of Sciences, Beijing 100049, China

Received 2012 March 30; accepted 2012 May 10

Abstract We collect the second Large Area Telescope AGN catalog (2LAC) and Monitor of Jets in AGN with VLBA Equipment (MOJAVE) quasi-simultaneous data to investigate the radio-γ connection of blazars. The cross sample contains 166 sources. The statistical analysis based on this sample confirms positive correlations between these two bands, but the correlations become weaker as the γ-ray energy increases. The statistical results between various parameters show negative correlations of γ-ray photon spectral index with γ-ray loudness for both Flat Spectrum Radio Quasars (FSRQs) and BL Lacertae objects, positive correlations of γ-ray variability index with the γ-ray loudness for FSRQs, a negative correlation of the γ-ray variability index with the γ-ray photon spectral index for FSRQs, and negative correlations of γ-ray photon spectral index with γ-ray luminosity for FSRQs. These results suggest that the γ-ray variability may be due to changes inside the γ-ray emission region like the injected power, rather than changes in the photon density of the external radiation fields, and the variability amplitude tends to be larger as the γ-rays are closer to the high energy peak of the spectral energy distribution (SED). No correlation of variability index found for BL Lacertae objects implies that variability behavior may differ below and above the peak energy.

Key words: BL Lacertae objects: general — galaxies: jets — quasars: general — radio continuum: galaxies — gamma rays: observations

1 INTRODUCTION

Blazars, the most extreme class of Active Galactic Nuclei (AGNs), are observed in almost the full electromagnetic spectrum from radio to the γ-ray band. They contain two subclasses called BL Lacertae objects (BL Lacs) and Flat Spectrum Radio Quasars (FSRQs). The radiation from blazars

* Supported by the National Natural Science Foundation of China.

is believed to be the non-thermal emission of relativistic jets with small viewing angles with respect to the line of sight (Urry & Padovani 1995). The broadband spectral energy distribution (SED) shows two components in the $\nu - \nu F_\nu$ diagram. The lower energy component that peaks in the infrared to X-ray band is believed to be produced by the synchrotron process of relativistic electrons. The radiation mechanism of the higher energy component has been more debatable until now. It is generally believed that the γ-ray emission is produced by the inverse Compton (IC) process of the same electron population that emits the synchrotron emission (e.g., Maraschi et al. 1992; Sikora et al. 1994). This indicates a connection between radio and γ-ray emission, but the connection could be indirect because the emission regions of radio and γ-ray may be different due to synchrotron self-absorption. Moreover, some observations found the connection between these two bands, at least during the flare period, e.g., the γ-ray flares occur after the ejections of new superluminal components (Jorstad et al. 2001). However, the location of γ-ray emission regions and the source of seed photons are still uncertain (Marscher et al. 2010; León-Tavares et al. 2011; Tavecchio et al. 2010), and why only a small fraction of blazars are γ-ray loud is still an open question (e.g., Kovalev et al. 2009; Linford et al. 2011; Sikora et al. 2002).

The connection between radio and γ-ray emission can help us constrain the radiation process and the emission region in the jets, especially for the γ-ray band. This has been considered since the EGRET era, but no confirmed conclusion had been made due to the limits of the sensitivity of the telescope and the erratic sample (Kovalev et al. 2009). Thanks to the high sensitivity, broad energy range, and large field of view in the Large Area Telescope (LAT, Atwood et al. 2009) onboard the Fermi Gamma Ray Space Telescope (Fermi) successfully launched in 2008, a much larger sample and more accurate measures for photon fluxes and spectra can be achieved. Many papers have investigated the connection between these two bands, and almost all of them confirmed a positive correlation in Fermi blazars (Kovalev et al. 2009; Ghirlanda et al. 2010, 2011; Linford et al. 2011, 2012; Ackermann et al. 2011a). However, these previous results showed many different behaviors in different subclasses or energy bands. Moreover, these studies only used non-quasi-simultaneous data, or only studied the correlation between radio flux and γ-ray flux, and both of them depend on distance.

After a two year survey of LAT, the second LAT AGN catalog (2LAC) gives a more accurate classification and association of 1121 AGNs in γ-rays, and 886 sources in its clean sample (Ackermann et al. 2011b). Some radio monitoring programs are operating in the Fermi era at different frequencies, e.g., the MOJAVE (Monitor of Jets in AGN with VLBA Equipment, Lister et al. 2009) program at 15 GHz, the OVRO (Owens Valley Radio Observation, Richards et al. 2011) program at 15 GHz, UMRAO (the University of Michigan Radio Variability Program) at 4.8, 8.0, and 14.5 GHz, and so on. These programs give us a good chance for investigating the connection between radio and γ-ray emission with quasi-simultaneous data.

Nolan et al. (2012) obtained the spectral index of γ-ray photons fitted with a single power-law and the γ-ray variability index, which shows the level of γ-ray variability. The spectral index is often discussed in research, as it reflects the peak of the SED (e.g., Ghisellini et al. 2009; Lister et al. 2011). It is possible that the variability index is also important for investigating the location of the γ-ray emission region and the origin of γ-ray variability. Ackermann et al. (2011a) has discussed it in the γ-ray range for the 2LAC clean sample.

In this paper, we statistically analyze both flux and luminosity correlations with the quasi-simultaneous data of 2LAC and MOJAVE for the first time. The data of seven different γ-ray energy bands are used to study the dependence of the radio-γ connection on γ-ray energy bands. The γ-radio luminosity ratio is defined as a parameter of γ-ray loudness (Arshakian et al. 2012; Lister et al. 2011). Then we examine the correlations of γ-ray photon spectral index and the γ-ray variability index with the γ-radio luminosity ratio and other parameters in our sample.

In Section 2, we describe our sample and data; Section 3 presents the methods we use and the results; Section 4 gives discussion and a summary. In this paper, we use a ΛCDM cosmology model

with $h = 0.71$, $\Omega_m = 0.27$ and $\Omega_\Lambda = 0.73$ (Komatsu et al. 2009). We define the radio spectral index as $S(\nu) \propto \nu^{-\alpha}$, and the γ-ray photon spectral index as $dN/dE \propto E^{-\Gamma}$.

2 SAMPLE AND DATA

We choose the sources of the 2LAC clean sample which have been monitored by the MOJAVE program. For the quasi-simultaneous data, we require a time interval matching the Fermi data (from 2008-08-04 to 2010-08-01, Nolan et al. 2012). Considering the gap of the radio monitoring data, and the probable time lag between the variabilities of these two bands, we use a broad time interval for radio data during 2008-01 to 2011-04. In order to perform the K-correction and luminosity calculations, we reject the sources without redshift data. Finally, our sample contains 166 sources, with 127 FSRQs and 39 BL Lacs (hereafter cross sample). For FSRQs, there are 119 low synchrotron peaked blazars (LSPs), and 8 sources without SED classification. For BL Lacs, there are 7 high synchrotron peaked blazars (HSPs), 13 intermediate synchrotron peaked blazars (ISPs), 18 LSPs, and 1 source without SED classification. The classification and redshift data of our cross sample are from 2LAC (Ackermann et al. 2011b). The K-corrections for radio flux and γ-ray photon flux are calculated as

$$S_{\nu_0} = S^{'}_{\nu_0}(1+z)^{\alpha+1} \tag{1}$$

and

$$N(E_1, E_2) = N^{'}(E_1, E_2)(1+z)^{\Gamma-1}, \tag{2}$$

respectively. The radio and γ-ray luminosity are calculated by the observed flux as

$$L_{\nu_0} = 4 \times 10^{-26} \pi d_L^2 S^{'}_{\nu_0}(1+z)^{\alpha-1} \qquad \mathrm{erg\ s^{-1}\ Hz^{-1}} \tag{3}$$

and (Ghisellini et al. 2009)

$$L(\nu_1, \nu_2) = 4\pi d_L^2 S^{'}(\nu_1, \nu_2)(1+z)^{\Gamma-2} \qquad \mathrm{erg\ s^{-1}}, \tag{4}$$

respectively. In Equations (3) and (4), d_L is the luminosity distance, and $S^{'}(\nu_1, \nu_2)$ is the γ-ray energy flux observed between frequencies ν_1 and ν_2 which correspond to the energies E_1 and E_2, respectively. $S^{'}(\nu_1, \nu_2)$ is derived as

$$S^{'}(\nu_1, \nu_2) = \frac{(1-\Gamma)h\nu_1 N^{'}(E_1, E_2)[(\frac{\nu_2}{\nu_1})^{2-\Gamma} - 1]}{(2-\Gamma)[(\frac{\nu_2}{\nu_1})^{1-\Gamma} - 1]} \quad \mathrm{erg\ s^{-1}\ cm^{-2}}, \quad \Gamma \neq 2. \tag{5}$$

Due to the absence of quasi-simultaneous data of the radio spectral index, and the generally flat radio spectrum for blazars, we assume that the radio spectral index is equal to 0 for the sources in our sample.

For Fermi data, we use the 1–100 GeV photon flux in 2LAC (Ackermann et al. 2011b), and the 100–300 MeV, 300 MeV–1 GeV, 1–3 GeV and 3–10 GeV data in the second Fermi-LAT catalog (2FGL, Nolan et al. 2012). For upper limits, we directly use them for our analysis (Ackermann et al. 2011a), but we remove the 10–100 GeV data because too many sources only have upper limits in this band. We obtain the 100 MeV–1 GeV photon flux combined with the 100–300 MeV and 300 MeV–1 GeV data, as well as the 100 MeV–100 GeV photon flux combined with the 100–300 MeV, 300 MeV–1 GeV and 1–100 GeV data. For MOJAVE data, we use the mean value of all the VLBA observations for each source.

3 RESULT

We use the nonparametric Spearman test for our correlation analysis, except that the luminosity correlation is tested by partial correlation analysis to remove the dependence on redshift. In this paper, we define a significant correlation when the chance probability is less than 0.001.

The data of 15 GHz radio flux and the γ-ray photon flux (100 MeV–100 GeV) are plotted in Figure 1. The Spearman test confirms the positive correlation of radio and γ-ray flux, though the correlation has a certain dispersion. This means that the sources with higher radio flux always have higher γ-ray flux. The correlation for BL Lacs seems to be better than that for FSRQs. The correlation coefficient and chance probability are 0.38 and 1.1×10^{-5} for FSRQs, and 0.44 and 0.006 for BL Lacs, respectively.

Then we examine the correlations between the photon flux of each individual γ-ray energy band and the radio flux. The correlations become worse when the energy band increases, especially for BL Lacs (see Table 1). This indicates that the connection between radio and γ-ray emission weakens as the γ-ray energy increases. There are no correlations of the radio flux with those of 1–3 GeV, 3–10 GeV or 1–100 GeV for BL Lacs. Otherwise, for other bands including 100 MeV–100 GeV, the correlation coefficients of BL Lacs are larger than those of FSRQs. For the radio and gamma-ray luminosity, we find positive correlations in all energy bands with the correlation coefficients of BL Lacs larger than those of FSRQs (Fig. 2). Correlation coefficients decrease when γ-ray energy increases. Figure 3 shows the changes in correlations with four energy bands, 100–300 MeV, 300 MeV–1 GeV, 1–3 GeV and 3–10 GeV.

Figure 4 shows the plot of the γ-ray photon spectral index versus the γ-radio luminosity ratio (100 MeV–100 GeV). BL Lacs and FSRQs have a similar range in γ-ray loudness, and both of them have negative correlations between the γ-ray photon spectral index and the γ-ray loudness in most γ-ray energy bands, with the correlations for BL Lacs better than those for FSRQs. For FSRQs, we find positive correlations between the γ-radio luminosity ratio and γ-ray variability index (Fig. 5). The γ-ray variability index is negatively correlated with the γ-ray photon spectral index for FSRQs (Fig. 6).

We also examine the correlations of radio flux and luminosity versus γ-ray photon spectral index and γ-ray variability index, respectively. We find the same trends for flux and luminosity. They have good correlations of radio flux and luminosity versus γ-ray photon spectral index for BL Lacs,

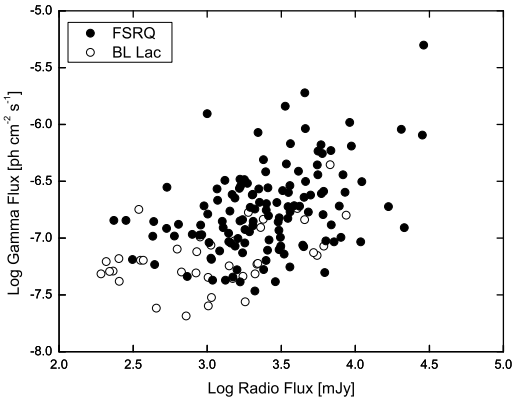

Fig. 1 15 GHz radio flux versus γ-ray photon flux (100 MeV–100 GeV). The filled circles represent FSRQs and the open ones represent BL Lacs.

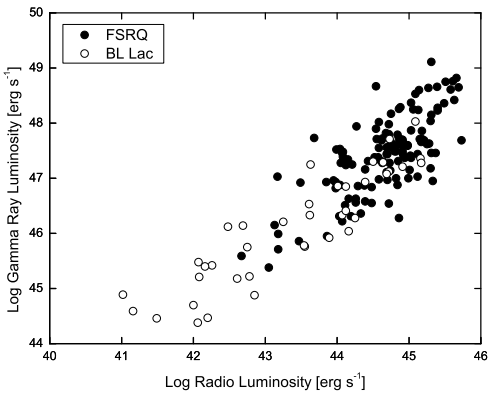

Fig. 2 15 GHz radio luminosity versus integrated γ-ray luminosity (100 MeV–100 GeV). The symbols are the same as in Fig. 1.

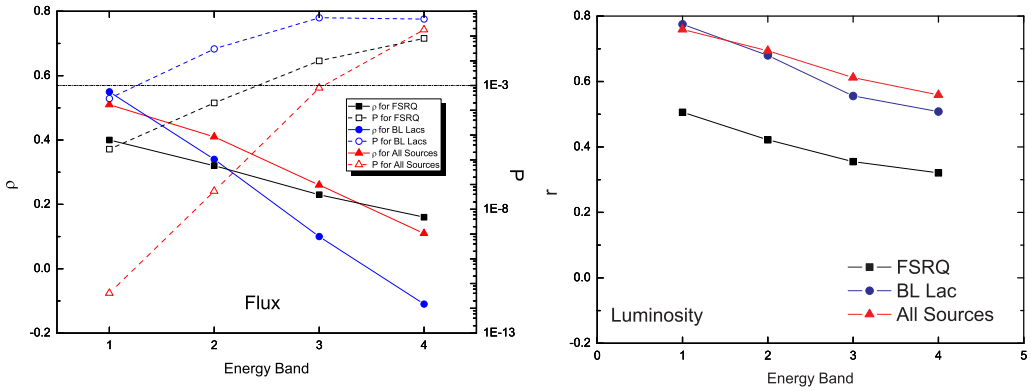

Fig. 3 Changes of correlations with energy bands. The black filled squares represent correlation coefficients for FSRQs, the blue filled circles represent correlation coefficients for BL Lacs, the red filled triangles represent correlation coefficients for all sources in our cross sample, and the open ones represent the chance probabilities (*color online*). *Left* shows the change of flux correlations, and the dot-dashed line represents a chance probability of 0.001. *Right* shows the change of partial correlation coefficients for luminosity. The corresponding chance probabilities are almost all less than 0.001, and only one is 0.001.

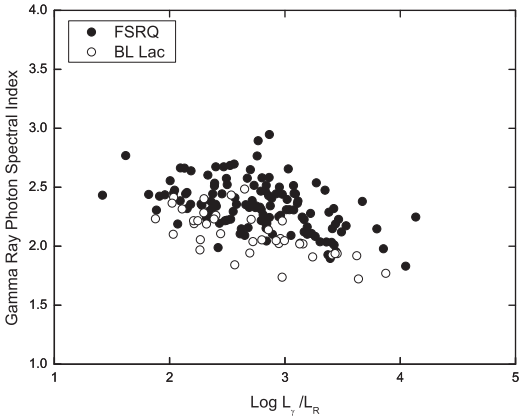

Fig. 4 The γ-radio luminosity ratio (γ-ray luminosity is from 100 MeV to 100 GeV) versus γ-ray photon spectral index. The symbols are the same as in Fig. 1.

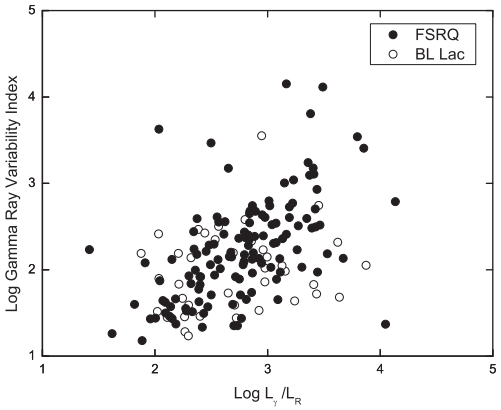

Fig. 5 The γ-radio luminosity ratio (γ-ray luminosity is from 100 MeV to 100 GeV) versus γ-ray variability index. The symbols are the same as in Fig. 1.

respectively. There are no correlations of radio flux and luminosity versus gamma-ray photon spectral index for FSRQs. There are no correlations of the radio flux and luminosity versus the γ-ray variability index (see Table 2). For the γ-ray luminosity of each individual energy band versus the γ-ray photon spectral index and the γ-ray variability index, we find positive correlations between the γ-ray luminosity and the variability index for FSRQs (see Table 1), faint positive correlations between the γ-ray luminosity and the photon spectral index for BL Lacs, and weak negative correlations between the γ-ray luminosity and the photon spectral index for FSRQs, especially in the GeV band (see Fig. 7). All the correlation coefficients and chance probabilities are listed in Tables 1 and 2.

Table 1 Results of the Correlation Test with Seven Different γ-ray Energy Bands

Source Class			Energy Band (GeV)						
			$0.1< E <100$	$0.1< E <0.3$	$0.3< E <1$	$0.1< E <1$	$1< E <3$	$3< E <10$	$1< E <100$
FSRQ	F_R vs F_γ	ρ	0.38	0.4	0.32	0.39	0.23	0.16	0.21
		P	1.1E–5	2.7E–6	2E–4	6.5E–6	0.01	0.08	0.02
	L_R vs L_γ	r	0.39	0.51	0.42	0.48	0.36	0.32	0.28
		P	< 0.001	< 0.001	< 0.001	< 0.001	< 0.001	< 0.001	0.001
	L_γ vs Γ	ρ	-0.26	-0.03	-0.18	-0.1	-0.3	-0.37	-0.43
		P	0.003	0.7	0.05	0.28	8E–4	2.1E–5	4.1E–7
	$\frac{L_\gamma}{L_R}$ vs Γ	ρ	-0.47	-0.19	-0.38	-0.28	-0.5	-0.55	-0.61
		P	3E–8	0.03	1.3E–5	0.001	2.7E–9	1.9E–11	2E–14
	L_γ vs $TS_{\rm var}$	ρ	0.35	0.26	0.34	0.3	0.38	0.36	0.44
		P	5.9E–5	0.003	7.6E–5	7E–4	9.8E–6	2.7E–5	2.8E–7
	$\frac{L_\gamma}{L_R}$ vs $TS_{\rm var}$	ρ	0.59	0.49	0.58	0.52	0.6	0.55	0.63
		P	3.9E–13	6.3E–9	8.8E–13	2.9E–10	8E–14	2.2E–11	1.9E–15
BL Lac	F_R vs F_γ	ρ	0.44	0.55	0.34	0.49	0.1	-0.11	0.04
		P	0.006	3E–4	0.03	0.002	0.55	0.49	0.8
	L_R vs L_γ	r	0.58	0.78	0.68	0.74	0.56	0.51	0.43
		P	< 0.001	< 0.001	< 0.001	< 0.001	< 0.001	0.001	0.007
	L_γ vs Γ	ρ	0.42	0.55	0.51	0.53	0.43	0.41	0.35
		P	0.008	3E–4	0.001	6E–4	0.006	0.009	0.03
	$\frac{L_\gamma}{L_R}$ vs Γ	ρ	-0.72	-0.46	-0.52	-0.54	-0.64	-0.73	-0.77
		P	2.5E–7	0.003	7E–4	5E–4	1E–5	1.32E–7	7.6E–9
	L_γ vs $TS_{\rm var}$	ρ	0.09	0.05	0.11	0.08	0.14	0.12	0.15
		P	0.57	0.78	0.51	0.65	0.4	0.47	0.38
	$\frac{L_\gamma}{L_R}$ vs $TS_{\rm var}$	ρ	0.2	0.15	0.2	0.19	0.28	0.17	0.26
		P	0.23	0.36	0.21	0.24	0.09	0.29	0.12
All Sources	F_R vs F_γ	ρ	0.47	0.51	0.41	0.49	0.26	0.11	0.22
		P	1.2E–10	4.1E–12	5.4E–8	3.1E–11	8E–4	0.18	0.004
	L_R vs L_γ	r	0.64	0.76	0.69	0.74	0.61	0.56	0.5
		P	< 0.001	< 0.001	< 0.001	< 0.001	< 0.001	< 0.001	< 0.001
	L_γ vs Γ	ρ	0.1	0.27	0.17	0.23	0.07	0.02	-0.04
		P	0.21	4E–4	0.03	0.004	0.35	0.85	0.6
	$\frac{L_\gamma}{L_R}$ vs Γ	ρ	-0.43	-0.09	-0.28	-0.19	-0.45	-0.56	-0.6
		P	6.2E–9	0.23	3E–4	0.01	1.3E–9	8E–15	1.3E–17
	L_γ vs $TS_{\rm var}$	ρ	0.37	0.3	0.37	0.33	0.4	0.37	0.44
		P	1.2E–6	7.6E–5	1.3E–6	1.6E–5	1.1E–7	7.1E–7	3.7E–9
	$\frac{L_\gamma}{L_R}$ vs $TS_{\rm var}$	ρ	0.5	0.45	0.51	0.47	0.52	0.43	0.52
		P	7E–12	1.3E–9	1.4E–12	1.3E–10	6.4E–13	7E–9	4.9E–13

Notes: ρ is the correlation coefficient of the Spearman test, r is the correlation coefficient of the partial correlation analysis, and P is the chance probability.

Table 2 Results of the Correlation Test

Source Class	F_R vs Γ		L_R vs Γ		F_R vs $TS_{\rm var}$		L_R vs $TS_{\rm var}$		Γ vs $TS_{\rm var}$	
	ρ	P	ρ	P	ρ	P	ρ	P	ρ	P
FSRQ	0.11	0.22	0.08	0.36	0.01	0.94	-0.03	0.72	-0.47	2.8E–8
BL Lac	0.68	2.5E–6	0.66	4.2E–6	0.12	0.49	0.02	0.89	-0.18	0.27
All Sources	0.3	6.9E–5	0.34	6.2E–6	0.1	0.21	0.08	0.32	0.28	2E–4

Notes: ρ is the correlation coefficient of the Spearman test, and P is the chance probability.

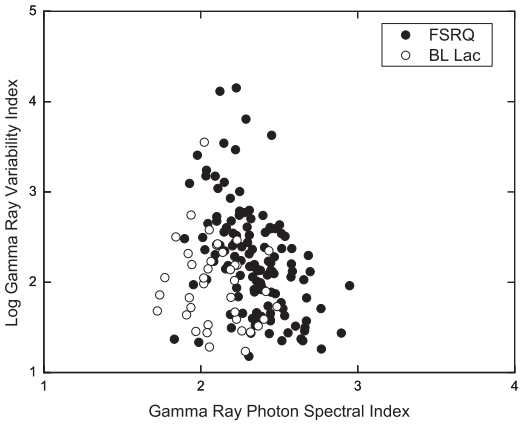

Fig. 6 The γ-ray photon spectral index versus γ-ray variability index. The symbols are the same as in Fig. 1.

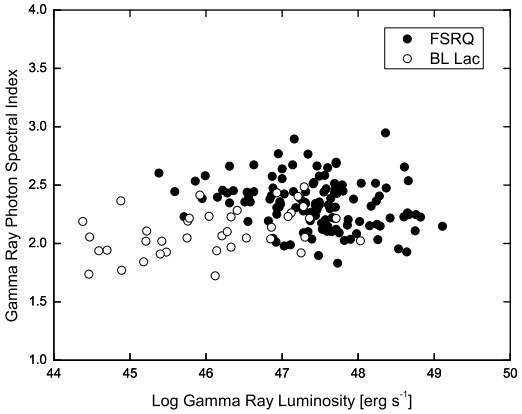

Fig. 7 The integrated γ-ray luminosity (100 MeV–100 GeV) versus γ-ray photon spectral index. The symbols are the same as in Fig. 1.

4 DISCUSSION

For our cross sample, we perform the Kolmogorov-Smirnov (K-S) tests of the redshift distribution compared with the 2LAC clean sample and a full blazar sample, i.e., the bzcat blazar sample (Massaro et al. 2009). There is an intrinsic difference in the redshift distribution between the cross sample and the bzcat sample (D = 0.184, probability = 0.0005 for FSRQs, and D = 0.291, probability = 0.003 for BL Lacs). There is no obvious difference between the 2LAC clean sample and our cross sample (D = 0.045, probability = 0.991 for FSRQs, and D = 0.159, probability = 0.366 for BL Lacs, see Fig. 8). This means that there is an intrinsic difference in redshift distribution between the 2LAC clean sample and the bzcat sample, which may be caused by the limited number of γ-ray detected sources, or the special physical mechanisms in γ-ray sources.

There is no difference for FSRQs in terms of γ-ray photon spectral index distributions between our cross sample and the 2LAC clean sample (D = 0.068, probability = 0.78). For BL Lacs, the sources in our sample tend to have a softer γ-ray spectrum than those in the 2LAC clean sample (see Fig. 9). This may be caused by a small fraction of HSP BL Lacs in our sample, because HSPs are generally weaker than ISPs and LSPs at the radio band (Ackermann et al. 2011a). All the sources in our sample tend to have a higher variability index than the 2LAC sources (Fig. 10). This means that our sample selected more variable sources and brighter sources in the γ-ray band because the variable sources determined by the variability index must be both intrinsically variable and sufficiently bright (Ackermann et al. 2011b).

Ackermann et al. (2011a) found the different behaviors of different energy bands in terms of flux correlation. They found that BL Lacs exhibited larger ρ values than FSRQs in the full sample, but there was an opposite trend in the OVRO sample. In the OVRO sample, no correlation was found for BL Lacs above 1 GeV, which did not appear in the full sample. The different results of these three samples may be caused by the selection effects such as different redshift distributions or different proportions of HSPs, ISPs, and LSPs in different samples. So we are also reminded that the radio-γ connection, especially the flux correlation, should be used very carefully.

The luminosity correlations between radio and each individual γ-ray energy band are confirmed by our sample. However, both flux and luminosity correlation coefficients decrease as the γ-ray energy increases. For HSPs, the 15 GHz and the GeV emission would be produced by low energy electrons, and there would be good correlations in these bands. But for ISPs and LSPs, the emission

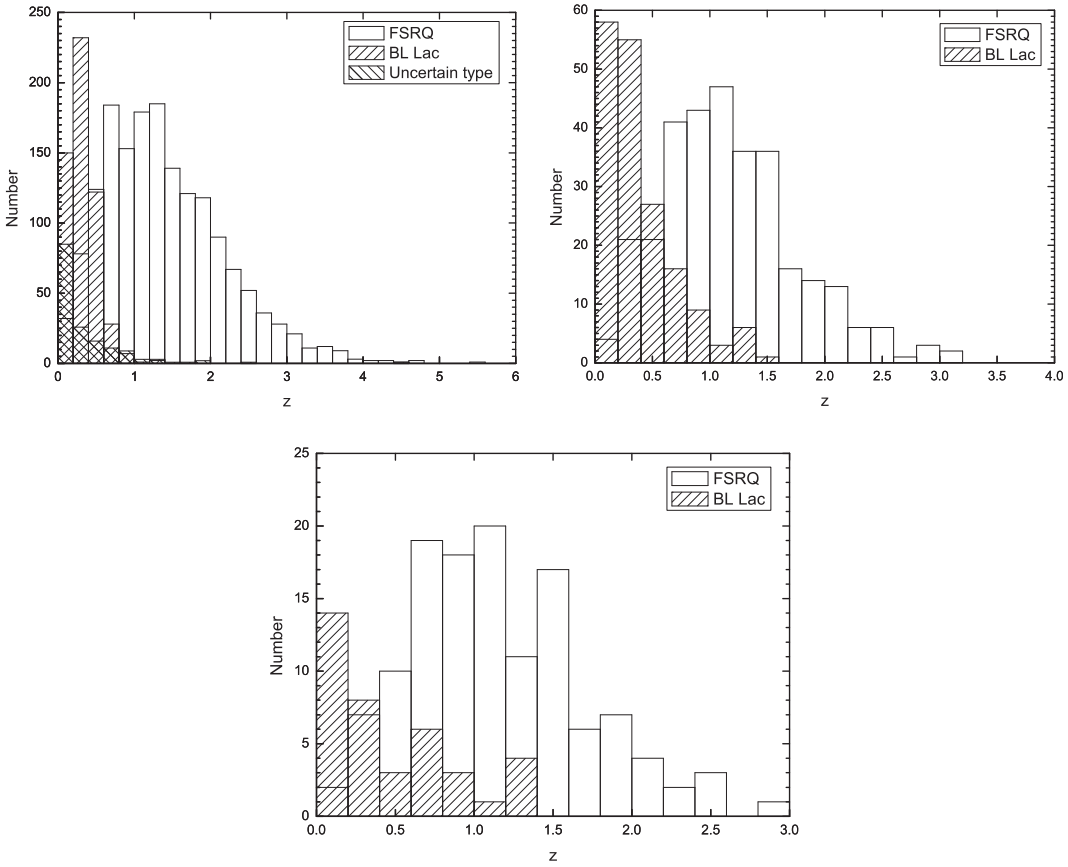

Fig. 8 The redshift distributions of three samples. *Upper left* is the bzcat blazar sample. *Upper right* is the 2LAC clean sample. *Bottom* is our cross sample.

of low energy electrons could only extend to the MeV band, and the correlations of radio and GeV bands would be weaker than those of radio and MeV bands. This would be the main reason why the correlation coefficients decrease as the γ-ray energy increases for both BL Lacs and FSRQs. Moreover, other mechanisms could also generate these trends, such as another radiation process or emission regions in the GeV band.

Lister et al. (2011) found a correlation between γ-ray loudness and γ-ray photon spectral index for BL Lacs, but no correlation for FSRQs. In our results, except for the energy below 1 GeV, both BL Lacs and FSRQs have negative correlations between the γ-ray loudness and the γ-ray photon spectral index. According to the average SEDs of the blazar sequence (Fossati et al. 1998), as the γ-ray spectrum becomes harder, i.e., the γ-ray photon spectral index decreases, the γ-ray peak of SED shifts to higher energy. At the same time, in the energy band of Fermi/LAT, the ratio of the γ-ray luminosity to the radio luminosity would increase significantly. Then it is expected that the γ-ray loudness is negatively correlated with the γ-ray photon spectral index. This expectation is consistent with our results. This trend is more remarkable among different subclasses for BL Lacs. For FSRQs, it becomes more remarkable as the energy is larger than 1 GeV (see Table 1). This is due to the effective cooling above the SED peak.

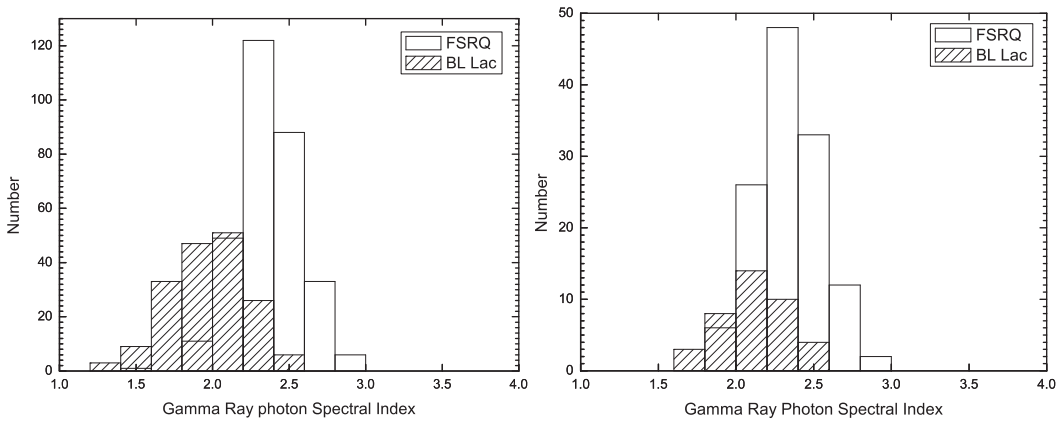

Fig. 9 The γ-ray photon spectral index distributions of the two samples. *Left* is the 2LAC clean sample. *Right* is our cross sample.

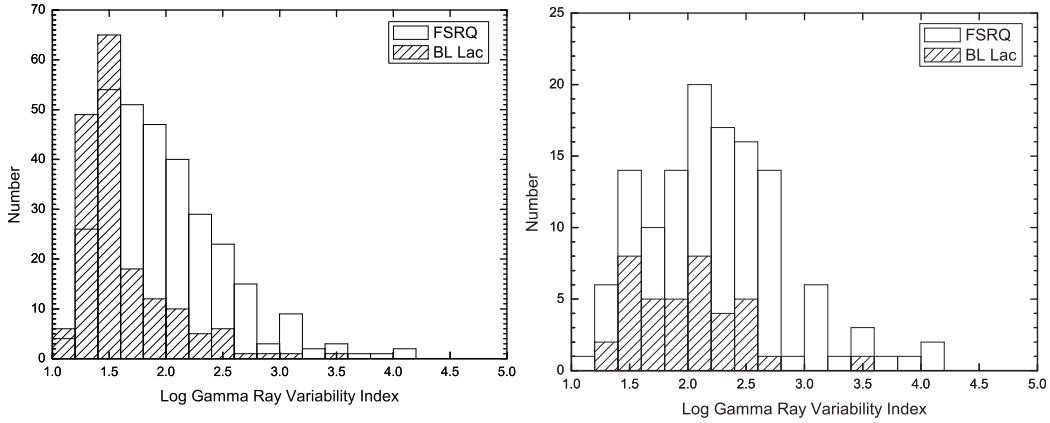

Fig. 10 The γ-ray variability index distributions of the two samples. *Left* is the 2LAC clean sample. *Right* is our cross sample.

The correlations between the γ-ray variability and the γ-radio luminosity ratio suggest that the variability, at least the main variability, could originate inside the γ-ray emission region like the changes of the injected power, because the changes in photon density of the external radiation field, such as variability in the accretion disk, could not affect the γ-ray loudness. This is opposite to the view of Paggi et al. (2011). These different trends of BL Lacs and FSRQs imply that variability behavior may differ below and above the peak energy (Ulrich et al. 1997; Ackermann et al. 2011b). As the γ-ray photon spectral index decreases, the high energy component shifts to the higher energy, and the γ-rays in the energy range of Fermi become closer to the high energy peak of SED for FSRQs. So the negative correlation of the γ-ray photon spectral index with the γ-ray variability index for FSRQs indicates that the amplitude of variability tends to be larger as the γ-rays move closer to the high energy peak of SED.

The correlations of radio and γ-ray luminosities with γ-ray photon spectral index for BL Lacs reflect the blazar sequence among different subclasses of BL Lacs (Fossati et al. 1998). For FSRQs, the negative correlation of γ-ray luminosity with γ-ray photon spectral index was also found in Ackermann et al. (2011b), where the correlation was very weak. In our results, the correlations become significant when the energy is larger than 1 GeV. These correlations would emerge if the more powerful sources have harder electron spectra. However, the fast decline above the high energy peak of SED could make the integrated luminosity of γ-rays smaller for the sources with a steeper γ-ray spectrum, even though the peak luminosity or the total luminosity is higher. This is consistent with the trend that the higher energy bands have better correlations (see Table 1). It is probable that our results, which seem opposite to the expectation of the blazar sequence, are caused by this reason. So as mentioned in Chen & Bai (2011), the γ-ray luminosity in the range of Fermi cannot simply be used to investigate the blazar sequence instead of the peak luminosity or the total luminosity, at least for FSRQs. The same trend of regarding harder when brighter is always observed in single sources, e.g., for 3C 454.3 (Abdo et al. 2011).

In summary, the radio and γ-ray emissions show a good connection in Fermi/LAT blazars, but these correlations become worse as the γ-ray energy increases. Moreover, the flux correlations would be affected strongly by the selection effects. The γ-ray variability index is correlated with other parameters for FSRQs. These correlations suggest that the γ-ray variability may be due to changes inside the γ-ray emission region like the injected power, rather than changes in the photon density of the external radiation field, and the variability amplitude tends to be larger as the γ-rays move closer to the high energy peak of SED. The different variability behaviors below and above the peak energy may cause different trends of BL Lacs and FSRQs. The negative correlations of the γ-ray luminosity with γ-ray photon spectral index suggest that the γ-ray luminosity in the range of Fermi cannot simply be used to investigate the blazar sequence instead of the the peak luminosity or the total luminosity, at least for FSRQs. However, our results are also limited by the number of sources in our sample, especially for BL Lacs. These results will be tested with larger samples.

Acknowledgements We thank the anonymous referee for insightful comments and constructive suggestions. We are grateful to Yibo Wang, Jiancheng Wang, Deliang Wang and Zunli Yuan for useful discussions. This research has made use of data from the MOJAVE database that is maintained by the MOJAVE team. We thank the National Natural Science Foundation of China (Grant Nos. 10903025, 10973034, 11103060 and 11133006) for financial support, and the support of the National Basic Research Program of China (973 Program, 2009CB824800).

References

Abdo, A. A., Ackermann, M., Ajello, M., et al. 2011, ApJ, 733, L26
Ackermann, M., Ajello, M., Allafort, A., et al. 2011a, ApJ, 741, 30
Ackermann, M., Ajello, M., Allafort, A., et al. 2011b, ApJ, 743, 171
Arshakian, T. G., León-Tavares, J., Böttcher, M., et al. 2012, A&A, 537, A32
Atwood, W. B., Abdo, A. A., Ackermann, M., et al. 2009, ApJ, 697, 1071
Chen, L., & Bai, J. M. 2011, ApJ, 735, 108
Fossati, G., Maraschi, L., Celotti, A., Comastri, A., & Ghisellini, G. 1998, MNRAS, 299, 433
Ghirlanda, G., Ghisellini, G., Tavecchio, F., & Foschini, L. 2010, MNRAS, 407, 791
Ghirlanda, G., Ghisellini, G., Tavecchio, F., Foschini, L., & Bonnoli, G. 2011, MNRAS, 413, 852
Ghisellini, G., Maraschi, L., & Tavecchio, F. 2009, MNRAS, 396, L105
Jorstad, S. G., Marscher, A. P., Mattox, J. R., et al. 2001, ApJ, 556, 738
Komatsu, E., Dunkley, J., Nolta, M. R., et al. 2009, ApJS, 180, 330
Kovalev, Y. Y., Aller, H. D., Aller, M. F., et al. 2009, ApJ, 696, L17
León-Tavares, J., Valtaoja, E., Tornikoski, M., Lähteenmäki, A., & Nieppola, E. 2011, A&A, 532, A146

Linford, J. D., Taylor, G. B., Romani, R. W., et al. 2011, ApJ, 726, 16
Linford, J. D., Taylor, G. B., Romani, R. W., et al. 2012, ApJ, 744, 177
Lister, M. L., Aller, H. D., Aller, M. F., et al. 2009, AJ, 137, 3718
Lister, M. L., Aller, M., Aller, H., et al. 2011, ApJ, 742, 27
Maraschi, L., Ghisellini, G., & Celotti, A. 1992, ApJ, 397, L5
Marscher, A. P., Jorstad, S. G., Larionov, V. M., et al. 2010, ApJ, 710, L126
Massaro, E., Giommi, P., Leto, C., et al. 2009, A&A, 495, 691
Nolan, P. L., Abdo, A. A., Ackermann, M., et al. 2012, ApJS, 199, 31
Paggi, A., Cavaliere, A., Vittorini, V., D'Ammando, F., & Tavani, M. 2011, ApJ, 736, 128
Richards, J. L., Max-Moerbeck, W., Pavlidou, V., et al. 2011, ApJS, 194, 29
Sikora, M., Begelman, M. C., & Rees, M. J. 1994, ApJ, 421, 153
Sikora, M., Błażejowski, M., Moderski, R., & Madejski, G. M. 2002, ApJ, 577, 78
Tavecchio, F., Ghisellini, G., Bonnoli, G., & Ghirlanda, G. 2010, MNRAS, 405, L94
Ulrich, M.-H., Maraschi, L., & Urry, C. M. 1997, ARA&A, 35, 445
Urry, C. M., & Padovani, P. 1995, PASP, 107, 803